

Effect of Temperature and Concentration on Self-Association of Octan-3-ol Studied by Vibrational Spectroscopy and Dielectric Measurements

Mirosław A. Czarnecki* and Kazimierz Orzechowski

Faculty of Chemistry, University of Wrocław, F. Joliot-Curie 14, 50-383 Wrocław, Poland

Received: June 26, 2002; In Final Form: December 4, 2002

The effects of temperature and concentration on self-association of octan-3-ol both in pure liquid and CCl₄ solution have been studied by two-dimensional (2D) Fourier transform near-infrared (FT-NIR) correlation spectroscopy, conventional FT-IR spectroscopy, and dielectric measurements. The interpretation of 2D correlation spectra was supported by simulation studies. A particular attention has been paid for comparison of the present results with that previously published for octan-1-ol. The obtained results indicate that population of the free OH groups changes faster than that of the associated species with increasing temperature. This results from the fact that in the open-chain multimers the terminal hydrogen bonds break easier than the interior ones. The open-chain dimers are less favorable than the higher associates due to the lack of the cooperativity effect. Hence, these species appear as a result of temperature-induced dissociation of higher multimers in concentrated solutions and in neat alcohols. At low concentration of alcohol in CCl₄ the nonpolar (cyclic) species dominates. An increase in the concentration of the sample increases the number and length of the linear associates, and this effect is more pronounced for primary alcohols. In octan-1-ol, formation of the linear associates is favored, whereas in octan-3-ol the cyclic species dominates. The present results reveal the presence of at least two kinds of associated species and argue against frequently assumed equilibrium between the monomers and one kind of associates at all concentrations.

Introduction

The effect of temperature and concentration on self-association of selected alcohols have been recently studied by generalized 2D FT-NIR correlation spectroscopy.^{1–7} Since the temperature and concentration affect the monomers and various associated species to different extent, the corresponding peaks appear as separate features in 2D asynchronous spectra, regardless of the separation in the normal spectrum. This resolution enhancement permitted the identification of a series of bands assigned to different vibrations of the free and bonded OH groups in the first and second overtone regions.^{1–7} The selective correlation of the peaks in the synchronous and asynchronous spectra makes the band assignment more reliable and gives an opportunity for reliable evaluation of anharmonicity constants.^{5,7}

The sign of the asynchronous peaks indicates which of the two dynamic spectral changes occurs earlier and which one occurs later.^{8,9} This property of the correlation spectra is a powerful tool for exploration of the molecular mechanism of perturbation-dependent changes in the studied system. However, the rules for interpretation of 2D correlation spectra were developed for the case, where two correlated signals vary with the same waveform. When the spectral responses follow completely different functions, the situations becomes more complicated and an application of the rules may lead to wrong conclusions.^{10–12} Hence, the comparison of dissimilar spectral responses has to be carefully performed. In this instance, the simulation studies are very helpful.

Previous 2D NIR correlation studies on self-association of alcohols indicate that the intensity changes for the monomers are slower than that of the associated species.^{1–7} This indicates

that the higher multimers at first break into shorter associates and then, at elevated temperatures, the shorter species dissociate into monomers. In this case the interior hydrogen bonds are expected to break easier than the terminal ones. However, this conclusion is not consistent with the theoretical studies on the stability of hydrogen bonding and role of the cooperativity effect in self-association of alcohols. *Ab initio* calculations demonstrate that the terminal hydrogen bonds are noticeable weaker than the interior ones.¹⁴ As can be seen (Figure 1), the dissociation of any kind of hydrogen-bonded species (processes A–E) leads to the increase in the population of the nonbonded OH groups. On the other hand, the changes in population of the higher multimers occur at slower rate. For example, the processes C and D produce the shorter chain associates, but for significant values of “*n*” these species still contribute to the “polymer” band (the lowest frequency band due to the associated species). Consequently, the intensity of the band arising from the free OH groups should vary faster than that assigned to the associates, contrary to previous reports on 2D correlation studies on alcohols.^{1–7} Obviously, the sign of asynchronous peaks for alcohols requires reexamination.

The asynchronous spectra of pure alcohols reveal a distinct peak near 6850 cm⁻¹, not resolved in the normal FT-NIR spectra.^{1–6} The position of this peak indicates that it originates from weakly bonded OH group. Following the same reasoning as that presented by Van Ness et al.,¹⁵ the feature at 6850 cm⁻¹ has been assigned to the cyclic dimers.^{2–7} However, there is still controversy over the structure of the dimeric species. The literature has both of the reports demonstrating that the dimers have cyclic^{15–18} and open^{19–23} structures. These discrepancies result from the fact that the molecular structure of the hydrogen-bonded species is not directly accessible from the vibrational spectra. This information may only be deduced from the spectra and it depends on assumed models and experimental conditions.

* To whom correspondence should be addressed. Faculty of Chemistry, University of Wrocław, F. Joliot-Curie 14, 50–383 Wrocław, Poland. Fax: 48–71–3282348. E-mail: mcza@wchuw.chem.uni.wroc.pl.

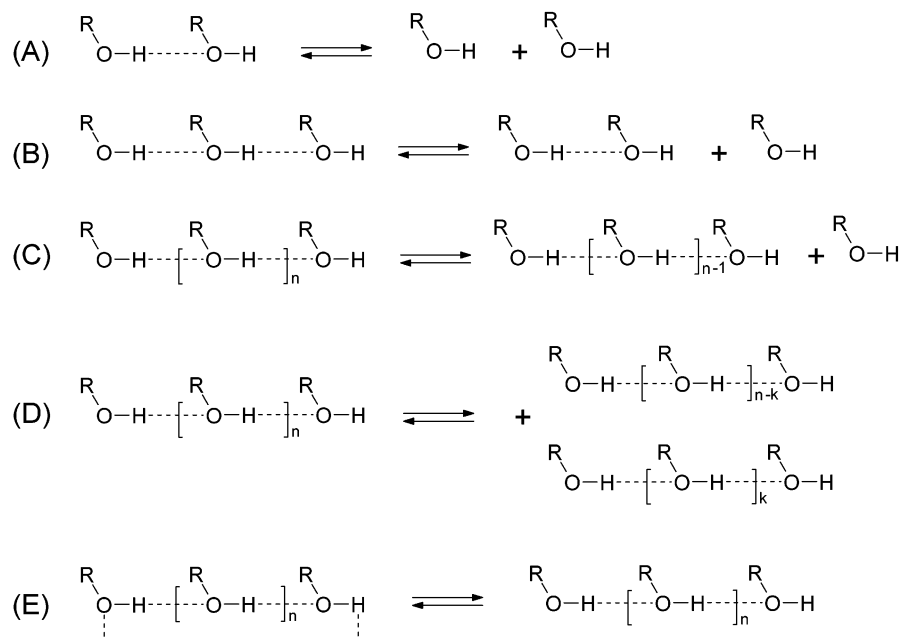


Figure 1. The dissociation pathways of hydrogen-bonded alcohols.

Therefore, the vibrational spectra of hydrogen-bonded systems should be discussed in connection with results of the theoretical calculations and different experimental techniques. The combination of vibrational and dielectric studies is particularly suitable for this purpose.^{24–26}

The present paper provides new experimental information on the effect of temperature and concentration on self-association of octan-3-ol by using 2D FT-NIR correlation analysis, conventional FT infrared (IR) spectroscopy, and dielectric measurements. The dielectric and FT-IR spectroscopic measurements were also performed for octan-1-ol. The interpretation of 2D correlation spectra was computer aided. The combination of FT-NIR and FT-IR spectroscopic measurements with dielectric studies made possible to gain a deeper insight into the molecular mechanism of self-association of alcohols and establish new assignments for some vibrational bands. The molar absorption coefficients for the fundamental, first, and second overtones of the monomer band were determined from the measurements at low concentrations. The obtained values were applied for the estimation of the fraction of nonbonded OH groups in the pure octan-3-ol and in CCl₄ solutions as a function of temperature. The comparison of present results with the analogous study on octan-1-ol^{6,7} permits the exploration of the effect of steric hindrance on the self-association of alcohols.

Experimental Section

Spectroscopic Measurements. Octan-1-ol, octan-3-ol, and CCl₄ were purchased from Aldrich Chemical Co. (Germany). The chemicals were obtained at the highest purity and were used as received. The purity of the samples was spectrally verified. The FT-IR and FT-NIR spectra were recorded at a resolution of 2 and 4 cm⁻¹, respectively, on a Nicolet Magna 860 spectrometer equipped with a DTGS detector and 512 scans were accumulated. The spectra of both octanols in CCl₄ were measured in a thermostated quartz cell (Hellma) of 10 or 100 mm thickness at 25 °C, while the spectra of pure octan-3-ol were recorded in a 1 or 5 mm cell in the temperature range of 20–80 °C with a stepwise increase of 5 °C. The actual temperature of the sample was controlled by means of a digital thermometer dipped into the cell, which guaranteed a stability of

±0.1 °C. The spectra recorded as a function of temperature were corrected for the density change with temperature, whereas the concentration-dependent spectra were concentration-normalized.²⁷

Dielectric Measurements. The electric properties were measured using a Hewlett-Packard bridge HP 4284A at the frequency 1 MHz. The capacitor was made of stainless steel and Teflon (air capacity was ≈5 pF). The relative accuracy of permittivity was estimated as ±0.1%. The temperature was stabilized by UNIPAN 650 controller and measured using calibrated thermocouple with the precision of ±0.1 K. The refractive index was measured for the sodium D line with Abbe refractometer with an accuracy of ±5 × 10⁻⁵. The density was measured pycnometrically with resolution of ±0.2 kg/m⁻³.

Data Processing. The synchronous intensity was calculated as a simple cross-product of the dynamic intensity at two different wavenumbers (ν_1 , ν_2), whereas the asynchronous intensity was computed as a cross-product of the dynamic intensity at ν_1 and Hilbert transform of the dynamic intensity at ν_2 .²⁸ In this study, the spectrum recorded at the lowest temperature or concentration was used as reference. To simplify interpretation of the asynchronous spectra, they were multiplied (array multiplication) by a sign of the corresponding synchronous spectra. In a synchronous spectrum, a positive peak at (ν_1 , ν_2) indicates that the intensity changes at these two wavenumbers are in the same direction. A positive asynchronous cross-peak at (ν_1 , ν_2) means that the spectral change at ν_1 occurs faster (earlier) than that at ν_2 . Negative synchronous and asynchronous peaks indicate the opposite. The 2D correlation analysis was performed by use of MATLAB 4.2 software (The Math Works, Inc.).

Results and Discussion

Simulation Studies. Figure 2 shows the relative intensity changes ($\Delta A_T = A_T - A_{20^\circ\text{C}}$) at 7093 (monomer band) and 6272 cm⁻¹ (“polymer” band) for pure octan-3-ol. The spectral responses for both bands occur in opposite direction and follow different waveforms. The changes for the “polymer” and monomer bands are approximated by polynomials of the first and second degree, respectively. It is also evident that the

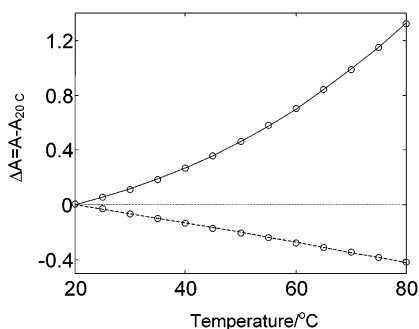


Figure 2. Temperature dependence of the relative absorbance of pure liquid octan-3-ol at 7095 and 6272 cm^{-1} (○). The solid and dashed lines represent the polynomials of the first and second degree fitting the intensity changes at 7095 and 6272 cm^{-1} , respectively.

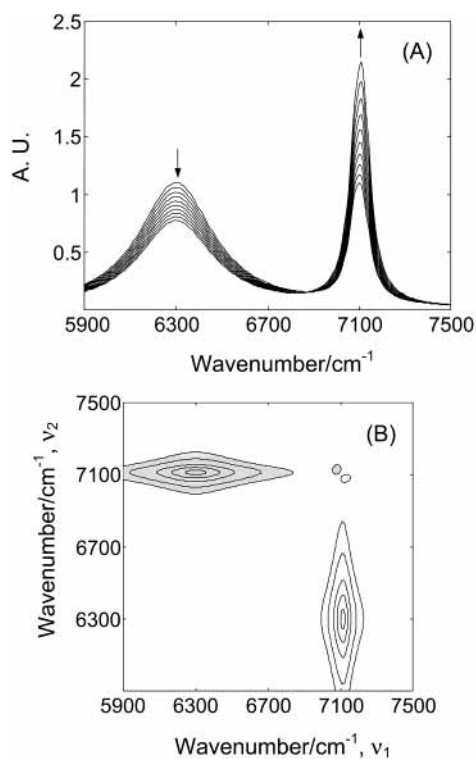


Figure 3. (A) The synthetic spectrum constructed from Lorentzian peaks located at 6300, 7080 and 7120 cm^{-1} . The intensity changes at 6300 and 7100 cm^{-1} vary according to the relationships at 6272 and 7095 cm^{-1} (see Figure 2), respectively. (B) The asynchronous spectrum calculated from the synthetic data. The negative peaks were shaded.

spectral changes for the monomer are faster than that of the associated species. The analogous situation takes place for the other alcohols.¹⁻⁷ The asynchronous spectra of most alcohols reveal two components in the region of the monomer band. Thus, the synthetic spectra were constructed from a broad band at 6300 cm^{-1} decreasing in intensity and two heavily overlapped bands at 7080 and 7120 cm^{-1} increasing in intensity (Figure 3A). The overall extent and rate of spectral changes for both apparent bands were the same as these for the monomer and “polymer” bands of octan-3-ol (Figure 2). Figure 3B shows the asynchronous spectrum constructed from the simulated data. The simulations were performed for different initial parameters (band position, width, height, and extent of the intensity changes), and the obtained results can be summarized as follows:

(1) The sign of the asynchronous peak at (6300, 7100 cm^{-1}) indicates that the spectral changes at 7100 cm^{-1} are faster than that at 6300 cm^{-1} .

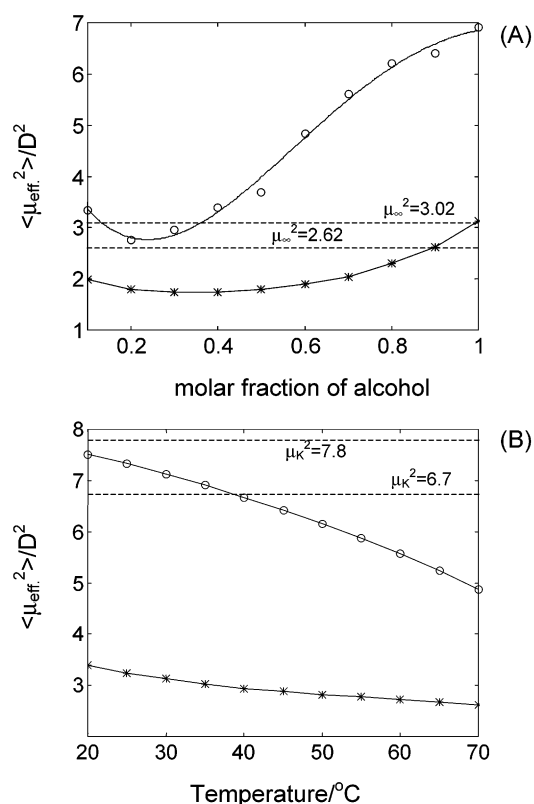


Figure 4. (A) The concentration dependence of $\langle \mu_{\text{eff}}^2 \rangle$ for octan-1-ol (○) and octan-3-ol (*) in CCl_4 at 25 °C. The dotted lines indicate the literature values determined for the diluted solution of octan-1-ol ($\mu_{\infty}^2 = 3.02 D^2$) and octan-3-ol ($\mu_{\infty}^2 = 2.62 D^2$). (B) The temperature dependence of $\langle \mu_{\text{eff}}^2 \rangle$ for pure octan-1-ol (○) and octan-3-ol (*). The dotted lines indicate the values determined from Kirkwood model for octan-1-ol ($\mu_K^2 = 7.8 D^2$) and octan-3-ol ($\mu_K^2 = 6.7 D^2$).

(2) The exact position of the asynchronous peak near 7100 cm^{-1} depends on the extent of the intensity changes for both components contributing to this band. If this extent is the same both at 7080 and 7120 cm^{-1} , the resulting peak is located at 7100 cm^{-1} , otherwise this peak shifts toward position of the component with larger extent of intensity changes.

(3) The separation between the 7080 and 7120 cm^{-1} peaks, obtained from the asynchronous spectrum, is always greater than the actual separation, as reported earlier.^{13,29,30}

From (2) and (3) results that the number of actual species is often smaller than the number of the asynchronous peaks. In Figure 3B one can identify four different peaks (at 6300, 7070, 7110, and 7130 cm^{-1}), whereas the original spectrum (Figure 3A) includes only three peaks (at 6300, 7080, and 7120 cm^{-1}).

Dielectric Measurements. The square of effective dipole moment ($\langle \mu_{\text{eff}}^2 \rangle$) was measured for octan-1-ol and octan-3-ol in CCl_4 as a function of concentration at constant temperature (Figure 4A) and in pure alcohols at different temperatures (Figure 4B). The apparent dipole moments were calculated from the measured permittivities, using the Onsager internal field.³¹ The variations in $\langle \mu_{\text{eff}}^2 \rangle$ with concentration are characteristic for solutions of alcohols in nonpolar solvents (Figure 4A).^{24-26,32,33} The dotted lines indicate the values of μ^2 determined for diluted solutions of octan-1-ol ($\mu_{\infty}^2 = 3.02 D^2$) and octan-3-ol ($\mu_{\infty}^2 = 2.62 D^2$).³⁴ The initial decrease in $\langle \mu_{\text{eff}}^2 \rangle$ was explained as a result of formation of the cyclic associates with a dipole moment close to zero.^{32,33} The degree of cyclization is significant for solutions of octan-3-ol in CCl_4 , while it seems to be smaller for solutions of octan-1-ol. The increase in $\langle \mu_{\text{eff}}^2 \rangle$ results from formation of highly polar (linear) associates and opening of the

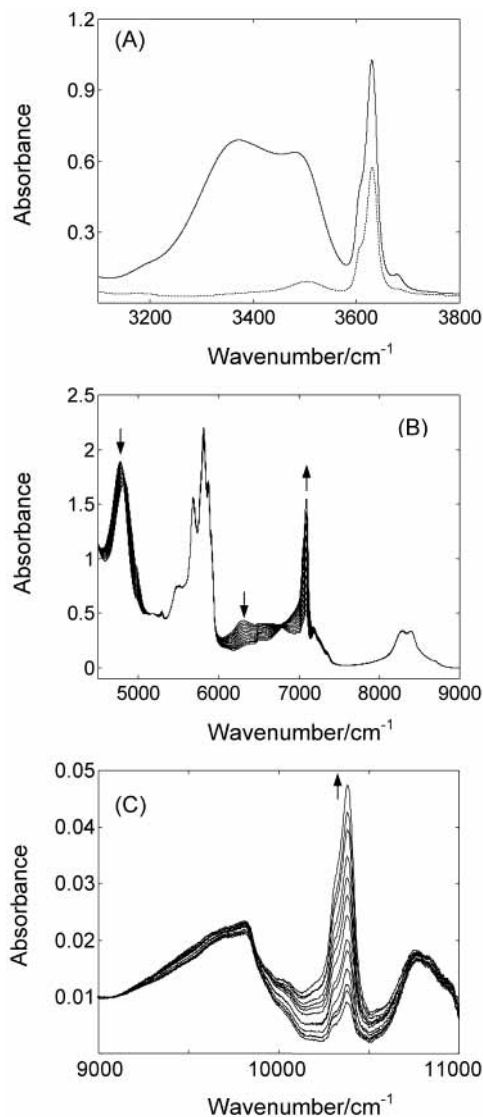


Figure 5. FT-IR spectra of octan-3-ol in CCl_4 at 1 M (solid line) and 0.2 M (dotted line) (A), FT-NIR spectra of pure octan-3-ol from 4500 to 9000 cm^{-1} (B) and from 9000 to 11000 cm^{-1} (C) over the temperature ranges of 20–80 °C (\uparrow , intensity increases; \downarrow , intensity decreases).

cyclic species. At moderate concentrations, the linear and cyclic associates coexist. In pure octanols the equilibrium is shifted toward formation of the linear associates, and this effect is more pronounced for octan-1-ol. The increase in temperature leads to the decrease in $\langle \mu_{\text{eff}}^2 \rangle$ (Figure 4B), but an extent of this effect is appreciably larger for octan-1-ol. This drop of $\langle \mu_{\text{eff}}^2 \rangle$ results mainly from reduction in the population and average size of the open-chain associates. For octan-3-ol the decrease in $\langle \mu_{\text{eff}}^2 \rangle$ is partially compensated by opening of the cyclic associates. It has been shown that the infinitely long hydrogen-bonded chain with free rotation about the hydrogen bond has a Kirkwood factor $g = 2.57$.³⁵ Hence, $\langle \mu_{\text{K}}^2 \rangle = \langle \mu_{\infty} \cdot g \rangle^2$ for octan-1-ol and octan-3-ol should take 7.8 and 6.7 D^2 , respectively. As can be seen (Figure 4B), $\langle \mu_{\text{eff}}^2 \rangle$ is much closer to the predicted value for pure octan-1-ol as compared to octan-3-ol. Hence, one can conclude that an average length of hydrogen-bonded chains is appreciably greater for primary octanol than that of secondary octanol.

Band Assignments. Figure 5A shows FT-IR spectra of octan-3-ol in CCl_4 at concentrations of 0.2 and 1 M, whereas Figures 5B,C display FT-NIR spectra of pure octan-3-ol in the range

TABLE 1: Frequencies and Assignments of Selected IR and NIR Bands of Octan-3-ol.

| vibration | species | position [cm^{-1}] |
|---------------------------------------|------------------|-------------------------------|
| $\nu(\text{OH})$ | higher multimers | 3371 |
| $\nu(\text{OH})$ | (cyclic trimer) | 3480 |
| $\nu(\text{OH})$ | free | 3630 |
| $\nu(\text{OH}) + \delta(\text{OH})$ | associated | ~ 4800 |
| $2\nu(\text{CH})$ | | 5681, 5813 |
| $2\nu(\text{OH})$ | higher multimers | 6272 |
| $\nu(\text{CH}) + \nu(\text{OH})$ | free | 6500 |
| $2\nu(\text{OH})$ | dimer | 6854 |
| $2\nu(\text{OH})$ | free | 7093 |
| $2\nu(\text{OH})$ | terminal free | 7033 |
| $2\nu(\text{CH}) + \delta(\text{CH})$ | | 7180 |
| $3\nu(\text{CH})$ | | 8285, 8387 |
| $3\nu(\text{CH}) + \delta(\text{CH})$ | | 9810 |
| $3\nu(\text{OH})$ | dimer | 9950 |
| $3\nu(\text{OH})$ | free | 10381 |
| $4\nu(\text{CH})$ | | 10805 |

^a In brackets are given positions of the rotational isomers.

20–80 °C in the low and high wavenumber regions, respectively. The positions and assignment of main spectral features in these regions are collected in Table 1. The combination band $\{\nu(\text{OH}) + \delta(\text{OH})\}$ shifts with temperature from 4773 to 4825 cm^{-1} (Figure 5B) giving rise to characteristic pattern in 2D correlation spectra.^{13,29,30} Thus, this band was not included into the analysis. The 2D-NIR correlation spectra of alcohols reveal two bands due to associated species. The first one is located near 6850 cm^{-1} and was assigned to the cyclic dimers.^{2–7} However, ab initio calculations demonstrate that the cyclic dimer is a transition state rather than a stable form.^{19,20} The 6850 cm^{-1} band is located relatively close to the monomer absorption, showing that the OH groups contributing to this band form weak hydrogen bonding. This weakness results from the absence of a cooperative effect for this species. The cooperative effects in hydrogen-bonded alcohols are reflected in shorter O–O distances, longer donor O–H bond lengths, larger energies per hydrogen bond, and greater shift of the donor O–H bond stretching frequencies than the dimer.^{36–38} The dimer is the only associates where the cooperative effect does not occur. Therefore, it seems reasonable to assign the band at 6850 cm^{-1} to the open dimer. This means that the remaining associated species (linear and cyclic) contribute to a broad peak centered near 6300 cm^{-1} . In fact, the internal hydrogen bonds in linear associates are not much different from these in the larger cyclic aggregates.¹⁵

In the literature one can find numerous reports assigning the fundamental band at 3350 cm^{-1} to the cyclic associates.^{16,17,39,40} Yet, the intensity of this band decreases with temperature rising (not shown). The decrease in the population of the cyclic species would increase $\langle \mu_{\text{eff}}^2 \rangle$, contrary to the observation presented here. Thus, we propose to assign the 3350 cm^{-1} band both to the open and cyclic multimers. The 3480 cm^{-1} band is frequently assigned to the dimeric species,^{19,20,22,41} yet the calculated anharmonicity constants $[(6854/2 - 3480) = -53 \text{ cm}^{-1}]$ are twice lower than the corresponding values for the dimer band (Table 3). Furthermore, these values are lower than those of the monomer band, making this assignment rather doubtful. Probably, the 3480 cm^{-1} band originates from short cyclic associates (like trimers), but a definite assignment of this band cannot be derived from present data.

Two-Dimensional Correlation Analysis of Temperature-Dependent Spectra of Octan-3-ol. An interesting information provides the comparison between the power spectra calculated in low (20–50 °C) and high (50–80 °C) temperature ranges (Figure 6). The power spectrum is a diagonal of the synchronous

TABLE 2: Molar Absorptivities of the $\nu(\text{OH})$, $2\nu(\text{OH})$, and $3\nu(\text{OH})$ of the Monomer Band for Octan-3-ol in CCl_4 at 25 °C Together with the Literature Data for Octan-1-ol

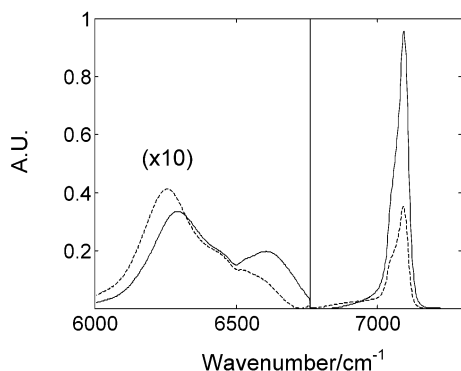
| alcohol | $\nu(\text{OH})$ | | $2\nu(\text{OH})$ | | $3\nu(\text{OH})$ | |
|------------|------------------|--------------------|--------------------------|----------------------------|------------------------|---------------|
| | int ^a | ph ^b | int | ph | int | ph |
| octan-3-ol | 1350 ± 20 | 43.9 ± 0.5 | 100.9 ± 1.0 | 1.52 ± 0.05 | 4.75 ± 0.2 | 0.050 ± 0.005 |
| octan-1-ol | 1670 ± 20 | 59.4 ± 0.5 | 107.0 ± 1.0 ⁶ | 1.78 ± 0.05 ⁶ | 5.4 ± 0.2 ⁶ | |
| | | 62.1 ⁴⁰ | | 1.65 ± 0.05 ^{47c} | | |
| | | | | 1.6 ^{45,a} | | |
| | | | | 1.68 ± 0.05 ^{48d} | | |

^a int: integrated, in $[\text{dm}^3 \cdot \text{mol}^{-1} \cdot \text{cm}^{-2}]$. ^b ph: at peak height, in $[\text{dm}^3 \cdot \text{mol}^{-1} \cdot \text{cm}^{-1}]$. ^c In decane. ^d In octane.

TABLE 3: Positions of the $\nu(\text{OH})$, $2\nu(\text{OH})$, and $3\nu(\text{OH})$ Bands for the Stretching Vibrations of the Free and Associated OH Groups of Octan-3-ol and Octan-1-ol⁷ Together with the Anharmonicity Constants (in Brackets)^a

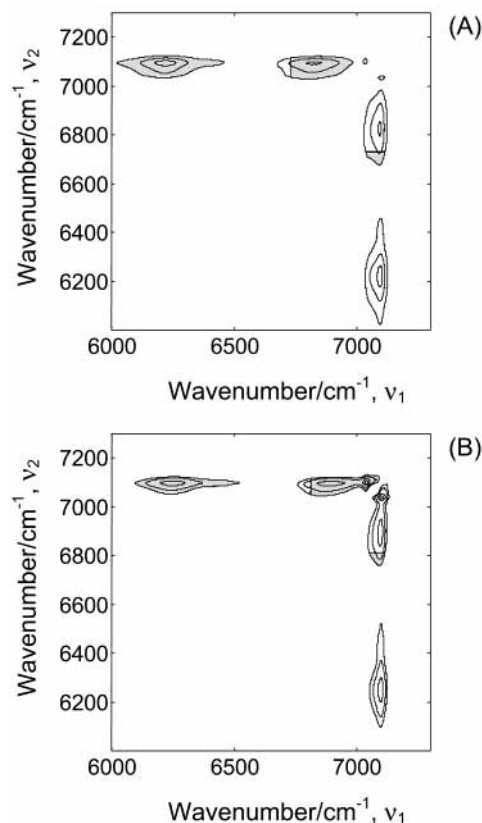
| species | $\nu(\text{OH})$ | | $2\nu(\text{OH})$ | | $3\nu(\text{OH})$ |
|-------------------------|------------------|----------|-------------------|---------|-------------------|
| octan-3-ol | | | | | |
| monomer ^a | 3631 | (−83.5) | 7095 | (−86.0) | 10384 |
| | 3606 | (−82.0) | 7048 | (−86.0) | 10314 |
| dimer | | | | | |
| higher multimers | 3371 | (−235) | 6742 | (−102) | 9974 |
| octan-1-ol ⁷ | | | | | |
| monomer ^b | 3639 | (−84.0) | 7110 | (−83.0) | 10415 |
| | 3628 | (−88.0) | 7080 | (−81.0) | 10377 |
| dimer | | | | | |
| higher multimers | 3345 | (−220.0) | 6250 | (−108) | 9950 |

^a All values are in cm^{-1} and an estimated accuracy is within $\pm 2 \text{ cm}^{-1}$ for monomer, $\pm 5 \text{ cm}^{-1}$ for dimer, and $\pm 10 \text{ cm}^{-1}$ for higher multimers. ^b The structure of the monomer band is due to the rotational isomerism.

**Figure 6.** Power spectra of pure octan-3-ol over the temperature ranges of 20–50 °C (dotted line) and 50–80 °C (solid line).

spectrum and represents the overall extent of intensity changes at individual wavenumbers. As can be seen (Figure 6), the population of the free OH groups increases faster at higher temperatures, while the fraction of higher multimers reveals an opposite trend. The position of the monomer band does not vary with temperature. In contrast, the “polymer” band strongly shifts toward higher wavenumbers as the temperature is increased, but its integrated intensity remains the same. This indicates that an average size of the associated species is decreased significantly, while the overall population of these species is reduced to smaller extent. The shape of the “polymer” band may suggest existence of additional peaks, yet the situation is complicated due to overlap with the $\nu_{\text{CH}} + \nu_{\text{OH}}$ combination mode ($\sim 6500 \text{ cm}^{-1}$) involving the free OH group.^{6,42,43}

Figure 7A,B displays the asynchronous spectra of pure octan-3-ol over the temperature ranges of 20–50 and 50–80 °C, respectively. The spectra develop an apparent asynchronicity between the monomer band and the bands due to the associated species. The sign of these peaks suggests that the spectral changes for the monomer are faster than those of the associated species, regardless of temperature interval. The splitting of the

**Figure 7.** Asynchronous 2D NIR correlation spectra of pure octan-3-ol over the temperature ranges of (A) 20–50 °C and (B) 50–80 °C. The negative peaks are shaded.

monomer band resulting from the rotational isomerism, hardly observed at lower temperatures, clearly appears in the high temperature range. The position of the high frequency rotational isomer in the asynchronous spectrum is much closer to the position of the monomer band in the synchronous spectrum. Taking into account the results of simulation studies, one can conclude that the extent of intensity changes for the higher frequency rotational isomer is larger.

In Figure 8 is shown the asynchronous spectrum of octan-3-ol in CCl_4 (1 M) from 25 to 60 °C. The analogous plot for 0.1 M solution (not shown) was similar. In the region of the monomer band one can find four features at 7033, 7080, 7101, and 7108 cm^{-1} , although there are expected not more than three peaks. Since the peaks are located close to the diagonal, their actual positions are shifted from the real positions.^{13,29,30} The situation is similar to that observed in the simulated spectra. Thus, one can conclude that the number of actual peaks in this spectral region is three, compared to two peaks observed in pure octan-3-ol (Figures 5 and 6). Two of these peaks are due to the rotational isomerism, whereas the third peak can be assigned to the nonbonded (terminal) OH groups in the open-chain associates. An average size of the linear associates in solutions

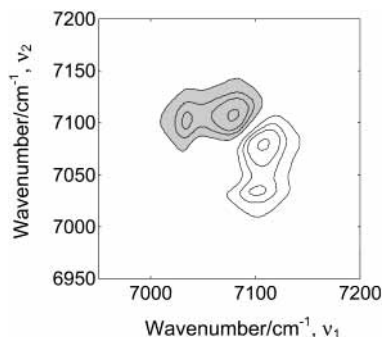


Figure 8. Asynchronous 2D NIR correlation spectrum of octan-3-ol in CCl_4 (1 M) from 25 to 60 °C. The negative peak is shaded.

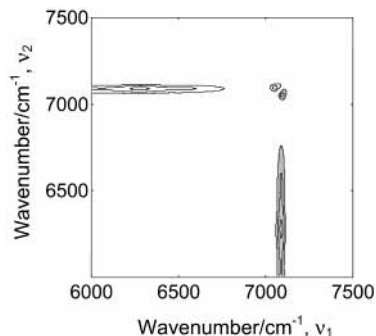


Figure 9. Asynchronous 2D NIR correlation spectrum of octan-3-ol in the concentration range 1.5–4.0 M at 25 °C. The negative peaks are shaded.

of octan-3-ol is smaller as compared to the liquid state. Thus, the population of the free terminal OH groups is high enough to develop a peak in the asynchronous spectrum (Figure 8). This peak was observed also in the spectra of other branched alcohols.^{2,3} As expected, the spectrum of octan-1-ol does not reveal the presence of nonbonded OH groups in the open-chain associates due to larger extent of association as compared with octan-3-ol.⁶

Two-Dimensional Correlation Analysis of Concentration-Dependent Spectra of Octan-3-ol. The asynchronous spectra of octan-3-ol in CCl_4 in the range of 1.5–4.0 M (Figure 9) and that of 0.1–1.0 M (not shown), reveal a significant intensity between the “polymer” and monomer band. In addition, one can observe a splitting of the monomer band due to the rotational isomerism. Of particular note is that the asynchronous spectra (in both concentration ranges) do not develop the open dimer peak, in contrast to the corresponding spectrum of pure octan-3-ol (Figure 6). The peak originating from the free terminal OH groups in the linear associates was not observed, as well. Both observations support the results of the dielectric measurements that formation of the cyclic species is strongly favored in this concentration range.

Rotational Isomerism of Octanols. Figure 10 displays deconvoluted spectra of octan-3-ol in CCl_4 (0.002 M) and in pure liquid state (6.3 M) in the region of the first overtone of the monomer band. Both spectra reveal two bands originating from the rotational isomers. At 0.002 M the self-association does not take place, and hence, the relative intensities of both bands reflect the differences in the energy and degeneracy of the rotational isomers. As expected, the higher frequency band is more intense (Figure 10A). Interestingly, the same tendency was found for pure octan-3-ol (Figure 10B), while the opposite effect was observed for primary alcohols.^{3,44} In Figure 11 are drawn the rotational isomers of octan-1-ol and octan-3-ol. In both cases, the positions I and III are equivalent, yet for octan-

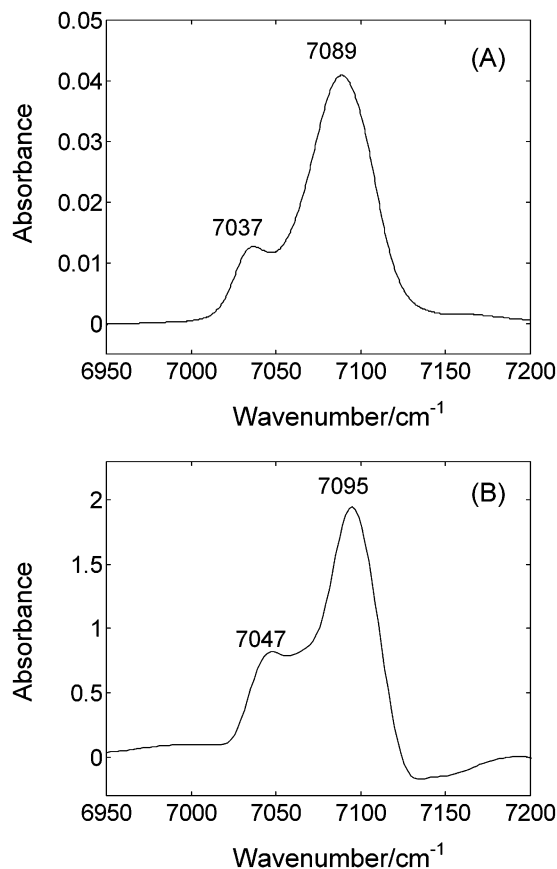


Figure 10. Deconvoluted spectra of octan-3-ol (A) in CCl_4 (0.002 M) and (B) in pure liquid phase (~ 6.3 M).

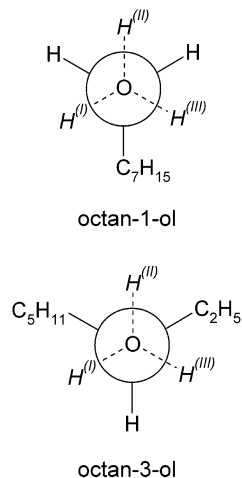


Figure 11. Rotational isomerism of octan-1-ol and octan-3-ol.

3-ol these positions are energetically more favorable as compared with position II, whereas for octan-1-ol is the opposite. The more stable rotamer is assigned to the high frequency band.² As previously discussed, for primary alcohols the hydrogen atom in position II is easier accessible than those in positions I and III.³ Thus, the higher fraction of hydrogen atoms in position II is predominantly engaged in hydrogen bonding and the corresponding band shows reduced intensity. For branched alcohols the population of both rotational conformers is determined mainly by the difference in values of the torsional potential and degeneracy, while the effect of hydrogen bonding seems to be less important. Therefore, for octan-3-ol, the higher frequency rotamer is more intense, regardless of the concentration.

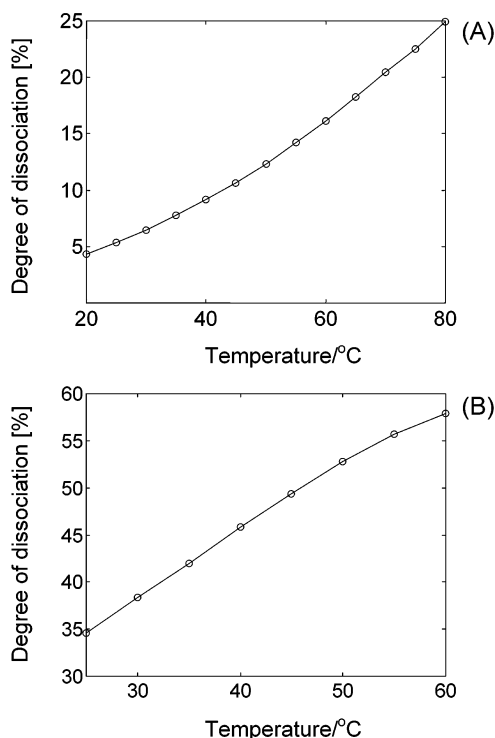


Figure 12. The temperature dependence of the degree of dissociation of (A) pure octan-3-ol and (B) 1 M solution in CCl_4 .

From Figure 11 results that the torsional potential of the OH group in positions I and III for octan-1-ol and octan-3-ol should be comparable. Indeed, the positions of the corresponding bands are similar ($\approx 7090 \text{ cm}^{-1}$). In contrast, the torsional potential in position II for both octanols differs significantly. As a result, the corresponding bands for octan-1-ol and octan-3-ol are located near 7110 and 7040 cm^{-1} , respectively. Obviously, the torsional potential significantly influences the frequency of the OH stretching vibration.

Determination of the Molar Absorption Coefficients of the $\nu(\text{OH})$, $2\nu(\text{OH})$, and $3\nu(\text{OH})$ for the Monomer Band. At low concentrations, alcohols occur in the monomeric form. Thus, from the measurements in diluted solutions one can determine the molar absorptivity of the monomer band (ϵ_M^{OH}). Numerous previous studies on alcohols show that ϵ_M^{OH} do not depend on temperature.^{44–47} The value of ϵ_M^{OH} was determined from the slope of the concentration-absorbance dependence. The measurements were performed in CCl_4 from 0.002 to 0.01 M at 25°C . In Table 2 are collected ϵ_M^{OH} for octan-3-ol together with the analogous values for octan-1-ol.^{6,40,45,47,48} As can be seen, the integrated ϵ_M^{OH} of the fundamental is 13–15 times higher than that of the first overtone, whereas the analogous ratio between the first and second overtones is 20. The corresponding values at peak height are noticeable greater (≈ 30). These discrepancies can be attributed to the rotational isomerism of the OH group. The integrated intensity of the monomer band does not depend on the rotational structure of this band, contrary to the values at a peak height. The ϵ_M^{OH} slightly decreases upon going from octan-1-ol to octan-3-ol. The same trend was observed for pentan-1-ol and pentan-3-ol.²¹

The Temperature Dependence of the Degree of Dissociation for Octan-3-ol in the Pure Liquid State and in CCl_4 Solution. The degree of dissociation, defined as a fraction of nonbonded OH groups [in %], was determined using the same method as previously.⁴⁴ As expected, the population of the free OH groups in pure octan-3-ol (Figure 12A) is appreciable higher

than that of octan-1-ol⁶ and decan-1-ol.⁴⁴ However, even at 80°C only 25% OH groups are nonbonded. The variation in the degree of dissociation with temperature for pure octan-3-ol is well approximated by the quadratic function. An extrapolation of this function to the melting (-15°C) and boiling point (175°C) yields 0% and 85%, respectively. In 1 M solution, the population of the free OH groups increases linearly up to 50°C , then the line bends and the increase becomes slower (Figure 12B). Interestingly, the degree of dissociation for 0.1 M solution ($\sim 83\%$) is temperature independent. As discussed, at lower concentrations predominantly exist more stable cyclic associates, and disruption of those species requires higher temperatures.

Anharmonicity of the $\nu(\text{OH})$ Vibration. The positions of the $\nu(\text{OH})$, $2\nu(\text{OH})$ and $3\nu(\text{OH})$ bands were used for determination of anharmonicity constants (χ^{OH}) for stretching vibrations of the free and associated OH groups (Table 3). The obtained values are compared with the corresponding data for octan-1-ol.⁷ The most characteristic tendency is an increase in χ^{OH} upon going from the monomer to higher associates. The values of χ^{OH} of the monomer band for both octanols are close to each other and are similar to those for other alcohols.^{6,49} The anharmonicity of the dimer is close to the analogous values for methanol in nitrogen (104.8 cm^{-1}) and argon (102.0 cm^{-1}) matrixes.⁵⁰ The large χ^{OH} for the “polymer” band may result from the fact that the relative intensities of the bands due to various associated species differ for the fundamental and first overtones.^{43,51}

Conclusions

Considering results both the dielectric and spectroscopic measurements one can draw following conclusions on self-association of octan-1-ol and octan-3-ol:

- (1) The dissociation of the higher associates into monomers does not occur directly but proceeds through the intermediate species.
- (2) Upon temperature rising the terminal hydrogen bonds break easier as compared to the internal ones. Thus, a fast increase in the population of the monomers is observed.
- (3) The temperature-induced shortening of an average size of the associates in the pure octan-1-ol does not significantly alter the population of the free terminal OH groups, and hence, the corresponding band is not observed in the correlation spectra. Yet, this process leads to decrease in $\langle u_{\text{eff}}^2 \rangle$ and therefore can be detected by dielectric measurements. In solutions, where an average size of the associates is smaller, the changes in population of the free terminal groups are more distinct.
- (4) Both an increase in temperature and decrease in concentration increase the population of the free OH groups at the expense of the bonded ones. Yet, the mechanism of these changes is different. The elevation of the temperature increases the fraction of the nonbonded OH groups in the linear associates, whereas the decrease in concentration does not have noticeable effect on the number of free terminal OH groups.
- (5) The dimers are less stable species as compared with the higher associates where the hydrogen bonding is stabilized by the cooperativity effect. Hence, the dimers do not appear upon an increase in the concentration of alcohol but are created during the thermal breaking of the higher associates in the pure liquid alcohols.
- (6) At moderate concentrations the cyclic species are created. Upon further increase in the concentration dominates the formation of the open-chain associates.
- (7) An average size and population of the linear associates are smaller in octan-3-ol as compared to octan-1-ol, while the

fraction of the free OH groups in pure secondary octanol is twice higher as that of primary octanol. This provides evidence that octan-3-ol shows reduced association as compared with octan-1-ol.

(8) The degree of the cyclization increases upon going from octan-1-ol to octan-3-ol at comparable concentrations.

(9) The obtained results evidence that from moderate concentrations to pure octan-3-ol exists the equilibrium between the monomers and two kinds of associated species: high dipole moment (linear) associates and low dipole moment (cyclic) ones.

(10) The torsional potential of the OH group about the CO axis has a significant effect on the frequency of the $\nu(\text{OH})$ vibration.

Acknowledgment. The authors gratefully acknowledge Magdalena Roszak (University of Wrocław) for assistance in measuring the FT-NIR spectra.

References and Notes

- Noda, I.; Liu, Y.; Ozaki, Y.; Czarnecki, M. A. *J. Phys. Chem.* **1995**, *99*, 3068.
- Czarnecki, M. A.; Maeda, M.; Ozaki, Y.; Suzuki, M.; Iwahashi, M. *Appl. Spectrosc.* **1998**, *52*, 994.
- Czarnecki, M. A.; Maeda, M.; Ozaki, Y.; Suzuki, M.; Iwahashi, M. *J. Phys. Chem. A* **1998**, *102*, 9117.
- Czarnecki, M. A.; Ozaki, Y. *Phys. Chem. Chem. Phys.* **1999**, *1*, 797.
- Czarnecki, M. A.; Czarnik-Matusiewicz, B.; Ozaki, Y.; Iwahashi, M. *J. Phys. Chem. A* **2000**, *104*, 4906.
- Czarnecki, M. A. *J. Phys. Chem. A* **2000**, *104*, 6356.
- Czarnecki, M. A. *Appl. Spectrosc.* **2000**, *54*, 1767.
- Noda, I. *Appl. Spectrosc.* **1990**, *44*, 550.
- Noda, I. *Appl. Spectrosc.* **1993**, *47*, 1329.
- Wang, H.; Palmer, R. A. In *Two-Dimensional Correlation Spectroscopy*; Ozaki, Y., Noda, I., Eds. AIP Conference Proceedings 503; American Institute of Physics: New York, 2000.
- Elmore, D. L.; Dluhy, R. A. *J. Phys. Chem. B* **2001**, *105*, 11377.
- Harrington, P. D.; Urbas, A.; Tandler, P. J. *Chemom. Intell. Lab. Syst.* **2000**, *50*, 149.
- Czarnecki, M. A. *Appl. Spectrosc.* **1998**, *52*, 1583.
- Hagemeister, F. C.; Gruenloh, C. J.; Zwier, T. S. *J. Phys. Chem. A* **1998**, *102*, 82.
- Van Ness, H. C.; Van Winkle, J.; Richtol, H. H.; Hollinger, H. B. *J. Phys. Chem.* **1967**, *71*, 1483.
- Liddel, U.; Becker, E. D. *Spectrochim. Acta* **1957**, *10A*, 70.
- Luck, W. A. P.; Schrems, O. *J. Mol. Struct.* **1980**, *60*, 333.
- Singh, S. S.; Rao, C. N. R. *J. Phys. Chem.* **1967**, *71*, 1074.
- Dixon, J. R.; George, W. O.; Hossain, M. F.; Lewis, R.; Price, J. M. *J. Chem. Soc., Faraday Trans.* **1997**, *93*, 3611.
- George, W. O.; Has, T.; Hossain, M. F.; Jones, B. F.; Lewis, R. J. *Chem. Soc., Faraday Trans.* **1998**, *94*, 2701.
- Shinomiya, K.; Shinomiya, T. *Bull. Chem. Soc. Jpn.* **1990**, *63*, 1093.
- Schwager, F.; Marand, E.; Davis, M. *J. Phys. Chem.* **1996**, *100*, 19268.
- Ehbrecht, M.; Huisken, F. *J. Phys. Chem. A* **1997**, *101*, 7768.
- Campbell, C.; Brink, G.; Glasser, L. *J. Phys. Chem.* **1975**, *79*, 660.
- Campbell, C.; Brink, G.; Glasser, L. *J. Phys. Chem.* **1976**, *80*, 686.
- Brink, G.; Glasser, L. *J. Phys. Chem.* **1978**, *82*, 1000.
- Czarnecki, M. A. *Appl. Spectrosc.* **1999**, *53*, 1392.
- Noda, I. *Appl. Spectrosc.* **2000**, *54*, 994.
- Gericke, A.; Gadaleta, S. J.; Brauner, J. W.; Mendelsohn, R. *Biospectrosc.* **1996**, *2*, 341.
- Czarnecki, M. A. *Appl. Spectrosc.* **2000**, *54*, 986.
- Onsager, L. *J. Am. Chem. Soc.* **1936**, *59*, 1486.
- Jadzyn, J.; Małcki, J.; Prałat, K.; Kędziara, P.; Hoffman, J. *Acta Phys. Pol.* **1974**, *A46*, 451.
- Małcki, J. A. *Chem. Phys. Lett.* **1998**, *297*, 29.
- McClellan, A. L. *Tables of Experimental Dipole Moments*; Chevron Research Company, 1989; Vol. 3.
- Oster, G.; Kirkwood, J. G. *J. Chem. Phys.* **1943**, *11*, 175.
- Del Bene, J.; Pople, J. A. *J. Chem. Phys.* **1970**, *52*, 4858.
- Kleberg, H.; Klein, D.; Luck, W. A. P. *J. Phys. Chem.* **1987**, *91*, 3200.
- George, A. J. *An Introduction to Hydrogen Bonding*; Oxford University Press: Oxford, 1997.
- Forland, G. M.; Libnau, F. O.; Kvalheim, O. M.; Hoiland, H. *Appl. Spectrosc.* **1996**, *50*, 1264.
- Nodland, E. *Appl. Spectrosc.* **2000**, *54*, 1339.
- Kunst, M.; van Duijn, D.; Bordewijk, P. *Ber. Bunsen-Ges. Phys. Chem.* **1979**, *83*, 840.
- Bourderon, C.; Peron, J. J.; Sandorfy, C. *J. Phys. Chem.*, **1972**, *76*, 864.
- Sandorfy, C. In *The Hydrogen Bond—Recent Developments in Theory and Experiments*; North-Holland Publishing Co.: Amsterdam, 1976; Chapter 13, pp 615–654.
- Czarnecki, M. A.; Liu, Y.; Ozaki, Y.; Suzuki, M.; Iwahashi, M. *Spectrochim. Acta* **1995**, *51A*, 1005.
- Iwahashi, M.; Hayashi, Y.; Hachiya, N.; Matsuzawa, H.; Kobayashi, H. *J. Chem. Soc., Faraday Trans.* **1993**, *89*, 707.
- Fletcher, A. N.; Heller, C. A. *J. Phys. Chem.* **1967**, *71*, 3742.
- Fletcher, A. N. *J. Phys. Chem.* **1969**, *73*, 2217.
- Aveyard, R.; Briscoe, B. J.; Chapman, J. *J. Chem. Soc., Faraday Trans. 1* **1973**, *69*, 1772.
- Iwahashi, M.; Suzuki, M.; Katayama, N.; Matsuzawa, H.; Czarnecki, M. A.; Ozaki, Y.; Wakisaka, A. *Appl. Spectrosc.* **2000**, *54*, 268.
- Perchard, J. P.; Mielke, Z. *Chem. Phys.* **2001**, *264*, 221.
- Luck, W. A. P.; Ditter, W. *Ber. Bunsen-Ges. Phys. Chem.* **1968**, *72*, 365.